Chapter 1

Introduction

The active sites of copper proteins (Type-1, Type-2, Type-3, Cu_A, Cu_B and Cu_Z) are briefly discussed. An overview of synthetic models that mimic the Cu_A site is provided. Related to the synthetic models for the Cu_A site is the redox isomerization reaction between Cu^{II} μ-thiolate and Cu^{I} disulfide species. The redox interconversion of these copper complexes is described in detail including the different reported ways to exert control over this equilibrium. At the end of the chapter a short overview of the contents of this thesis is given.

1.1 Introduction

Biological systems contain many different enzymes that are able to catalyze reactions very fast and very efficiently. A large number of proteins possess one or more copper ions in their active site to catalyze reactions such as electron transfer and oxidation of organic substrates.[1] To understand in what way these processes can be so effective, synthetic models are used to gain more insight into how these reactions take place within the enzyme and to see whether we can learn from them for other catalytic processes. Study of these models allows for a closer look at the coordination chemistry that is involved in relation to the activity of the enzyme. Model studies have for instance contributed significantly to the understanding of dioxygen activation by copper proteins.[2, 3]

Copper proteins are classified into groups based on the structure of their active sites. In this chapter, the Type-1, Type-2, Type-3, Cu_A, Cu_B and Cu_Z active sites (Figure 1.1) are briefly discussed. Furthermore, an overview of reported synthetic models for the Cu_A site and the related equilibrium between Cu^{II} thiolate and Cu^{I} disulfide species is provided.

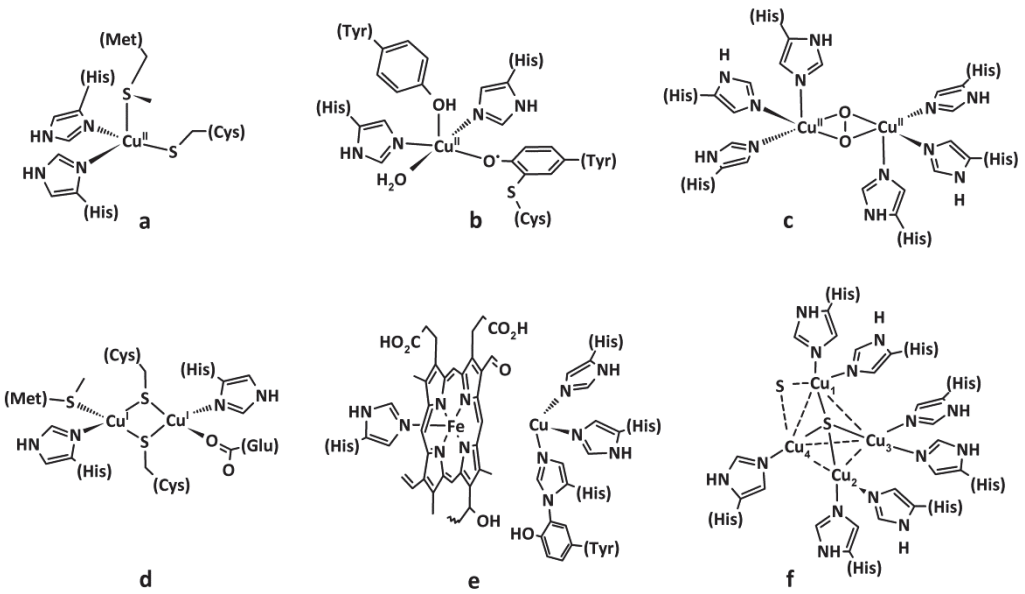

Figure 1.1: Schematic representation of the active sites of the copper proteins (a) plastocyanin (Type-1), (b) galactose oxidase (Type-2), (c) *oxy* hemocyanin (Type-3), (d) cytochrome *c* oxidase (Cu_A site), (e) cytochrome *c* oxidase (Cu_B site) and (f) N_2O reductase (Cu_Z site).

1.2 Copper proteins

1.2.1 Type-1 active site

Type-1 copper proteins are involved in electron-transfer processes and are found in mononuclear proteins such as azurin, amicyanin and plastocyanin (Figure 1.1a), but also in multicopper enzymes like ascorbate oxidase and nitrite reductase.[4] These proteins have an intense blue color due to the absorption band around 600 nm (ε = 5000 M^{-1} cm^{-1}; $Cu^{II} \leftarrow S_{cys}$ LMCT),[5] which is why these proteins are also called "blue copper proteins". These proteins are also characterized by their ground-state EPR signal, which has a unique small hyperfine coupling ($A_{\parallel} \approx 63 \times 10^{-4}$ cm^{-1}). The Cu^{II} ion in the active site has a distorted tetrahedral geometry, which comprises one equatorial, strongly coordinated S(Cys) residue (~2.1 Å), two N(His) ligands and one weakly coordinated axial ligand which is S(Met) in most cases, but can also be an oxygen of glutamine or leucine.

1.2.2 Type-2 active site

Type-2 copper proteins are often called "normal copper proteins", because the proteins lack distinctive spectroscopic features and have EPR features similar to 'common' Cu^{II} complexes containing an N,O chromophore with tetragonal geometry.[6, 7] The coordination sphere of the copper ion in the active site of these proteins consists of four N and/or O donors atoms in a square-pyramidal geometry. The open equatorial coordination position is usually filled by a water molecule. These proteins are predominantly involved in oxidation and oxygenation reactions in enzymes such as galactose oxidase (Figure 1.1b), Cu/Zn superoxide dismutase, amine oxidase and dopamine β-hydroxylase.[1]

1.2.3 Type-3 active site

This class of proteins comprises the enzymes hemocyanin, tyrosinase and catechol oxidase. These enzymes have an active site that contains two copper centers that can reversibly bind dioxygen in ambient conditions.[1] When dioxygen is bound to the enzyme (Figure 1.1c), the Cu^{II} ions are in such close proximity to each other, that they are anti-ferromagnetically coupled and are therefore EPR silent. Hemocyanin is an oxygen-transport protein in arthropods and mollusks, whereas tyrosinase and catechol oxidase bind dioxygen to oxidize phenolic substrates to catechol (tyrosinase) and successively to *o*-quinones (tyrosinase and catechol oxidase), which are then further used for the production of the pigment melanin. The catalytic mechanism by which catechol oxidase oxidizes *o*-bishydroxyarenes to *o*-quinones is still not

completely clarified,[8] but a schematic representation of the catalytic cycle that fits structural, spectroscopic and biochemical data is shown in Figure 1.2.[9]

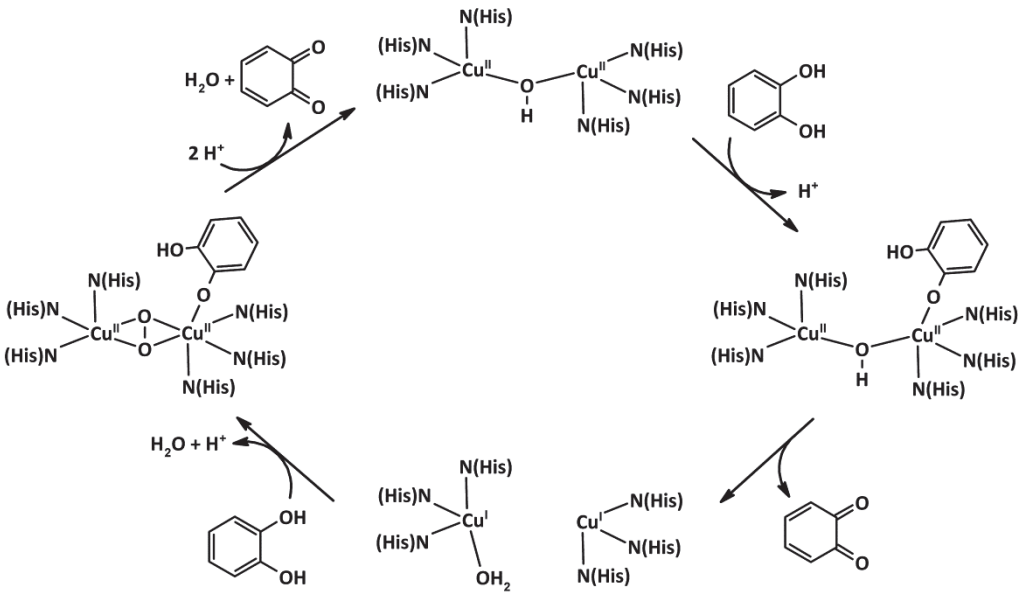

Figure 1.2: Catalytic cycle for the oxidation of catechol by catechol oxidase proposed by Sacchetini et.al.[9]

1.2.4 The Cu_A active site

Like the blue copper proteins, the Cu_A site is involved in electron transfer.[10] The Cu_A site shuttles electrons by varying the oxidation state of one of the two copper centers between Cu^I and Cu^{II} giving a formal oxidation state of $Cu^{1.5}$ in the oxidized state. The two copper ions are bridged by two cysteine thiolate moieties that together form a planar $Cu_2S(Cys)_2$ core with a Cu-Cu distance of ~2.44 Å in the oxidized $Cu^{1.5}Cu^{1.5}$ form and ~2.51 Å in the reduced form.[11] This indicates that there is a bond between the two copper centers, which was the first example of a metal-metal bond in nature.[12] The one-electron reduction of the Cu_A site results in only minor changes in the Cu_2S_2 core giving a slight increase of the Cu-S(Cys) bond from 2.3 Å to 2.33 Å. The Cu-S-Cu bond angles remain unchanged at 65°, which implies that only very low reorganizational energy is needed during electron transfer. Besides coordination to the two S(Cys) residues, each copper ion is coordinated to N(His) and either an S(Met) or a backbone peptide O (from Glu in C_cO and from Trp in N_2O reductase) (Figure 1.1d). The mixed-valence Cu_A site has a purple color and has a seven-line

hyperfine EPR pattern indicating delocalization of the unpaired electron over both copper centers.[13, 14] The Cu_A site is found in cytochrome *c* oxidase (C_cO)[15-17] and N_2O reductase.[18]

1.2.5 The Cu_B active site

In mitochondrial C_cO the electrons enter the Cu_A site (discussed in section 1.2.4) from cytochrome *c*, after which they are passed to the low-spin heme *a* center and subsequently to the high-spin heme a_3/Cu_B center. At this site, the electrons are used for the reduction of dioxygen to water, while generating a transmembrane proton pump that drives the synthesis of ATP.[19, 20] The heme a_3/Cu_B active site belongs to one (Type-A) of the three types of heme-copper oxidases and is the most well studied. The other two types are called Type-B and Type-C oxidases and have a similar active site, but differ in the subunit(s) surrounding the active site.[1, 21] The Cu_B site is located close to the iron center of the heme (~4.3 - 5.4 Å) and is coordinated to three N(His) residues with a vacant site directed towards the coordination sphere of the iron center (Figure 1.1e). Dioxygen is thought to bind between the copper center and the iron center.[22] The tyrosine residue that is covalently linked to a coordinating histidine residue plays a role in the dioxygen reduction.[23-25]

1.2.6 The Cu_Z active site

The Cu_Z active site comprises a tetranuclear copper cluster, which is found in N_2O reductase where it receives electrons from the Cu_A site (discussed in section 1.2.4) for the reduction of N_2O to N_2 and H_2O.[18, 26] The copper cluster is coordinated to seven N(His) residues and two sulfur ions, of which one is bridging all four copper ions (Figure 1.1f).[27] The catalytically active form contains four Cu^I ions. This form coordinates N_2O more easily than the Cu_Z resting state ($Cu^I_3Cu^{II}$).[28, 29]

1.3 Modeling of the Cu_A site

To gain a better understanding of how the rapid electron transfer within the Cu_A site occurs, synthetic models containing copper and bridging thiolate moieties have been designed. The synthesis of Cu^{II} thiolate complexes is complicated by the generally occurring redox reaction in which Cu^{II} is reduced to Cu^I,[30] as shown in equation (1).

$$2\ Cu^{II} + 2\ LS^- \rightarrow 2\ Cu^I + LSSL \qquad (1)$$

It is even more challenging to obtain a dinuclear copper μ-thiolate complex with a $Cu^{1.5}Cu^{1.5}$ oxidation state. Attempts initially led to the synthesis of mononuclear dithiolate Cu^{II} complexes,[31] mixed-valent multicopper complexes containing thiolate bridges,[32-34] dinuclear Cu^{II} complexes containing one thiolate bridge[35] and dinuclear Cu^{I} dithiolate complexes.[36, 37] The dinuclear Cu^{I} μ-thiolate complexes often contain a planar $Cu^{I}_2S_2$ core, like the Cu_A site, with a Cu-Cu distance that can be as small as 2.6 Å.[38, 39] An attempt has been made to oxidize a phenanthroline $Cu^{I}_2S_2$ complex to its mixed-valent state, but the oxidation showed irreversible behavior, although it was possible to form a mixed-valent $Cu^{0}Cu^{I}$ complex by electrochemical reduction.[39]

In 1995, the first dinuclear Cu^{II} dithiolate complex, depicted in Figure 1.3a, was reported by Tolman et.al.[40] Similar to the Cu_A site, this complex has Cu-S distances of ~2.33 Å, but the Cu-Cu distance is much larger with a distance of 3.34 Å. The Cu_2S_2 core has a 'butterfly' structure (Figure 1.3a), characterized by a 146.5° angle between the S-Cu-S planes. The complex displays intense UV-vis bands at 274, 338, 382 and 676 nm in methanol and is EPR-silent due to the anti-ferromagnetic coupling between the two Cu^{II} centers. Reduction to its mixed-valent state was not possible and only irreversible reductions were found with cyclic voltammetry. When the complex was dissolved in acetonitrile, an axial Cu^{II} EPR signal was observed indicating the formation of mononuclear species.

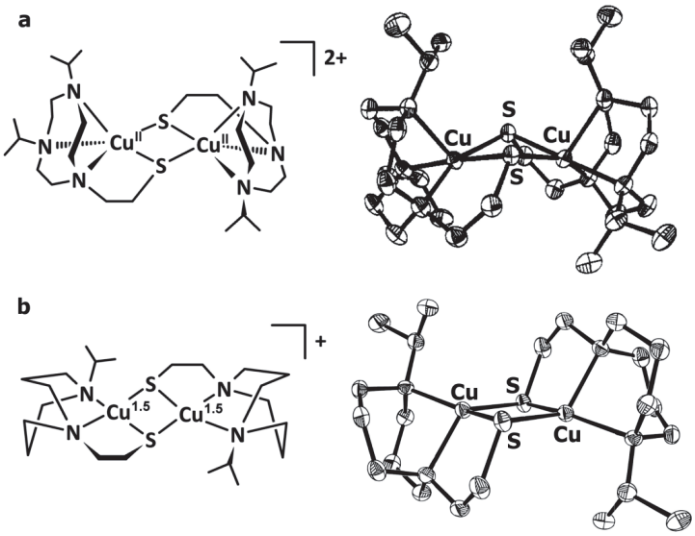

Figure 1.3: Schematic representations and displacement ellipsoid plots (50% probability level) of the cationic parts of (a) the Cu^{II} μ-thiolate complex and (b) $Cu^{1.5}$ μ-thiolate complex published by Tolman et.al.[40, 41] Hydrogen atoms are omitted for clarity.

After publication of the first Cu^{II} μ-thiolate complex, a number of dinuclear Cu^{II} thiolate complexes has been published with different ligands all containing additional nitrogen donors.[42-53] The Cu-Cu distance varies greatly from 2.65 Å[45] to 3.80 Å[53] and in most cases a similar 'butterfly' structure as in the Tolman Cu^{II} thiolate complex is observed (Figure 1.3a). An exception is the Cu^{II} μ-thiolate complex containing a pincer ligand, which has a planar Cu_2S_2 structure.[53]

The first $Cu^{1.5}Cu^{1.5}$ μ-thiolate complex was published one year after the first Cu^{II} thiolate structure.[41] The ligand used to obtain this complex is similar to the ligand in the Cu^{II} thiolate structure, except that it has one nitrogen donor less, generating four-coordinate Cu^{II} centers, similar to the Cu_A site (Figure 1.3b). The mixed-valent complex was synthesized from Cu^{II} and an excess of thiolate ligand, which was partially oxidized during the synthesis as shown in equation (2).

$$6\ LS^- + 4\ Cu^{II} \rightarrow 2\ [Cu^{1.5}{}_2(LS)_2]^+ + LSSL \qquad (2)$$

The mixed-valent complex shows more similarities to the Cu_A site than the Cu^{II} thiolate complexes. The Cu_2S_2 core is planar, with a Cu-Cu distance of 2.92 Å and the complex has an EPR signal consistent with a fully delocalized unpaired electron, as observed for the Cu_A resting state. The UV-vis absorption bands are slightly red-shifted and much less intense than those of the Cu_A site, possibly due to the larger Cu-Cu distance and the differences in donor atoms. Unfortunately, the system does not reproduce the reversible $Cu^ICu^I/Cu^{1.5}Cu^{1.5}$ redox behavior. In a more recent report the structures of both a Cu^ICu^I and $Cu^{1.5}Cu^{1.5}$ complex with the same ligand are discussed (Figure 1.4).[54] Both complexes are stable under inert atmosphere and can be inter-converted electrochemically, although oxidation to the $Cu^{II}Cu^{II}$ state results in complex decomposition. The dinuclear Cu^I complex is formed by a reaction of the precursor dithiolate ligand with dichloromethane, as shown in equation (3); the complex is oxidized with the mild oxidizing agent 4-bromobenzenediazonium tetrafluoridoborate to yield the $Cu^{1.5}Cu^{1.5}$ species.

$$2\ {}^-SLS^- + 2\ Cu^I + CH_2Cl_2 \rightarrow Cu^I{}_2(SLS\text{-}CH_2\text{-}SLS) + 2\ Cl^- \qquad (3)$$

Upon one-electron oxidation of the Cu^ICu^I species the Cu-Cu distance increases from 2.64 Å to 2.93 Å, cleaving the Cu-Cu bond, and flattening the 'butterfly' structure from a 153.1° angle to a 173.0° angle between the S-Cu-S planes (Figure 1.4).

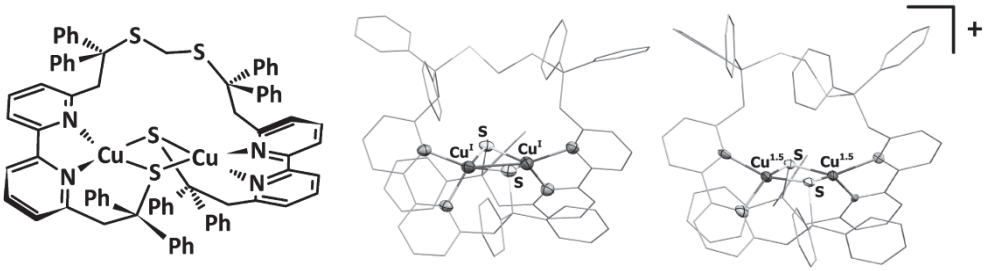

Figure 1.4: Schematic representation and projections of the cationic parts of the Cu^{II} μ-thiolate complex and $Cu^{1.5}$ μ-thiolate complex published by Duboc et.al.[54] Displacement ellipsoids are depicted at the 50% probability level. All hydrogen atoms are omitted, and a large part of the ligand is depicted in wireframe for clarity.

The $Cu^{1.5}Cu^{1.5}$ species has a purple color and shows the EPR signature of an unpaired electron delocalized over two copper centers. The electron self-exchange rate constant of the $Cu^{I}Cu^{I}/Cu^{1.5}Cu^{1.5}$ redox couple was measured to be k = 1.37(2) x 10^6 L mol^{-1} s^{-1},[55] which is faster than that of the Type-1 copper protein plastocyanin (k = 1.5 x 10^5 L mol^{-1} s^{-1}), but slower than that of the Cu_A site (k = 2.2 x 10^8 L mol^{-1} s^{-1}). According to the authors this is due to the cleavage of the Cu-Cu bond upon oxidation.
To date there is only one other report of a $Cu^{1.5}Cu^{1.5}$ complex, containing N-heterocyclic carbene ligands.[56] This species was only characterized in solution.

1.4 Cu^{II} thiolate and Cu^{I} disulfide equilibrium

1.4.1 General introduction

Research directed towards the synthesis of dinuclear Cu^{I}, $Cu^{1.5}$ and Cu^{II} thiolate complexes and their interconversion for mimicking the Cu_A site (section 1.3), has led to the discovery of a redox equilibrium. The redox reaction in which Cu^{II} and thiolate ligands are converted to Cu^{I} and disulfide ligands shown in equation 1, can also occur in the opposite direction depending on the ligand and the reaction conditions. Depending on the ligand set either a dinuclear Cu^{II} μ-thiolate or a Cu^{I} disulfide species can be formed and these species can be in equilibrium with each other. When the Cu^{I} disulfide complexes are converted to the Cu^{II} thiolate species a redox reaction takes place in which the electrons from the sulfur atoms are relocated, thus cleaving the S-S bond to form bridging thiolates and generating Cu^{II} ions. Because this reaction takes place intramolecularly the Cu^{II} thiolate and Cu^{I} disulfide species have the same charge, but different spectroscopic properties which makes it possible to distinguish

between both species. A schematic representation of this equilibrium is shown in Figure 1.5.

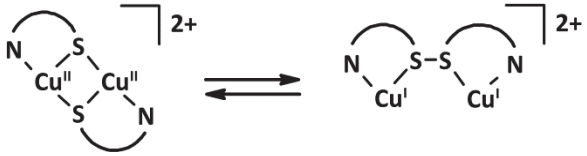

Figure 1.5: Schematic representation of the equilibrium between dinuclear Cu^{II} μ-thiolate and Cu^{I} disulfide complexes and their synthesis.

Investigating the Cu^{II} thiolate/Cu^{I} disulfide redox-equilibrium might provide a better understanding of the copper-sulfur redox reactions occurring in natural systems. Both species are more easily synthesized, compared to the rare mixed-valent $Cu^{1.5}$ complexes, giving the opportunity to study copper complexes with many different ligands. Furthermore, this equilibrium might provide information about other biologically occurring thiolate-disulfide reactions, involving molecules like cysteine and glutathione, that are tuned by the presence of a metal center.[57] For instance, the delivery of copper to the Cu_A site by Sco proteins is thought to occur by such a copper thiolate/disulfide conversion.[58-60] To get more information about the equilibrium it is necessary to be able to regulate the conversion in a controllable manner. This can be accomplished by changing the ligand or the reaction conditions.

1.4.2 Ligand-dependent conversion

The first paper to report both dinuclear Cu^{II} μ-thiolate and Cu^{I} disulfide species with a similar ligand was published in 2001.[46] It was shown that small structural changes in the ligand shift the formation of a Cu^{II} μ-thiolate species (**A**), to two different Cu^{I} disulfide complexes: a Cu^{I} *transoid*-disulfide species (**B**) and a Cu^{I} *cisoid*-disulfide species (**C**). A schematic overview of the complex syntheses starting from a disulfide ligand and two equivalents of Cu^{I} is shown in Figure 1.6.

The three different geometries were confirmed by X-ray structure determination. The Cu^{II} μ-thiolate complex is similar in geometry to other bis(μ-thiolato)dicopper(II) complexes with a Cu-Cu distance of 2.96 Å and a 'butterfly' structure with a 126.9° angle between the S-Cu-S planes. A small change in the R-groups of the ligand results in completely different geometries.

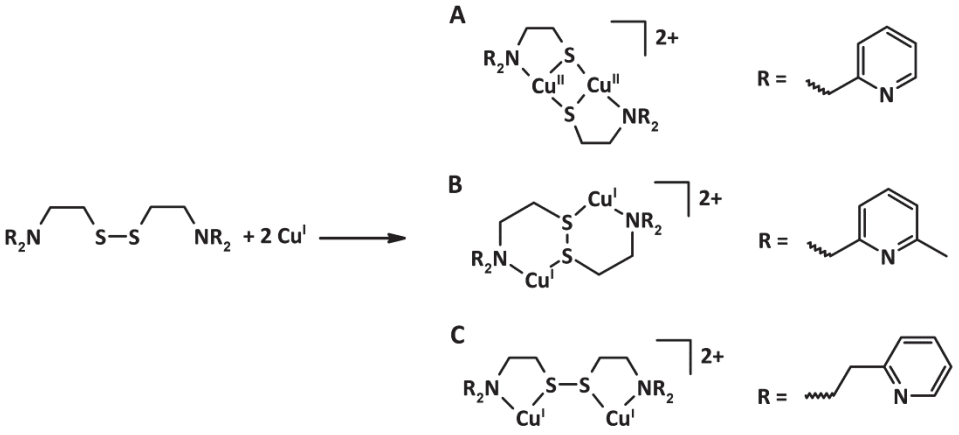

Figure 1.6: Schematic representation of the three different coordination geometries that can be formed starting from a disulfide ligand containing different R-groups and Cu^{I}.[46]

Replacing the methylene group between the tertiary amine and the pyridyl moiety with an ethylene group results in a Cu^{I} disulfide complex with geometry **C**. Geometry **C** is common for Cu^{I} disulfide complexes with the copper ions in a distorted tetrahedral geometry with a Cu-Cu distance of 3.91 Å. When a methyl group is added to the 6-position of the pyridyl moiety, Cu^{I} disulfide geometry **B** is formed. This structure is uncommon with its distorted trigonal pyramidal coordination sphere around the copper center and a large Cu-Cu distance of 5.16 Å. Geometry **B** can be seen as a potential intermediate geometry in going from **A** to **C**.

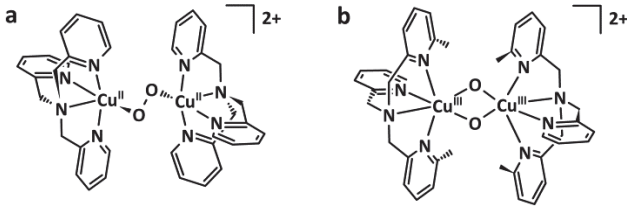

Figure 1.7: Schematic drawing of (a) a Cu^{II} μ-1,2-peroxo species with TPA ligand and (b) a Cu^{III} μ-oxido species with a TPA derived ligand.[61, 62]

It is worthy to note that a similar ligand change, where two 6-methyl groups are added to tris(2-pyridylmethyl)amine (TPA), also leads to a difference in geometry and redox state when the copper complex reacts with dioxygen. The compound $[Cu^{I}(TPA)(CH_3CN)]^{+}$ reacts with dioxygen to form a Cu^{II} μ-1,2-peroxo species,[61] while

the analogous copper complex coordinated to the dimethylated ligand forms a Cu^{III} μ-oxido species when exposed to dioxygen (Figure 1.7).[62] This change in geometry and oxidation states is completely opposite to those in **A** and **B**, indicating that geometry differences as a result of subtle ligand changes are difficult to generalize. The conversion of a Cu^{II} μ-1,2-peroxo species into a Cu^{III} μ-oxido complex was also reported to occur without a change in ligand structure.[63]

1.4.3 Chloride-induced conversion

The first Cu^{II} μ-thiolate to Cu^{I} disulfide conversion with the same ligand was reported to occur by the addition of chloride ions.[47] A ligand very similar to the ligands discussed in section 1.4.2. was reacted with Cu^{I} resulting in the formation of a Cu^{II} μ-thiolate species, even though the ligand provides only four instead of five coordination sites per copper center. Addition of one equivalent of Me_4NCl resulted in conversion to the Cu^{I} disulfide complex as indicated by a color change from dark brown to pale yellow. Addition of another equivalent of chloride anions led to small changes in the UV-vis spectrum and resulted in the formation of a bis(chlorido)dicopper(I) complex as is depicted in Figure 1.8a. The conversion was reversed by addition of $AgBF_4$.

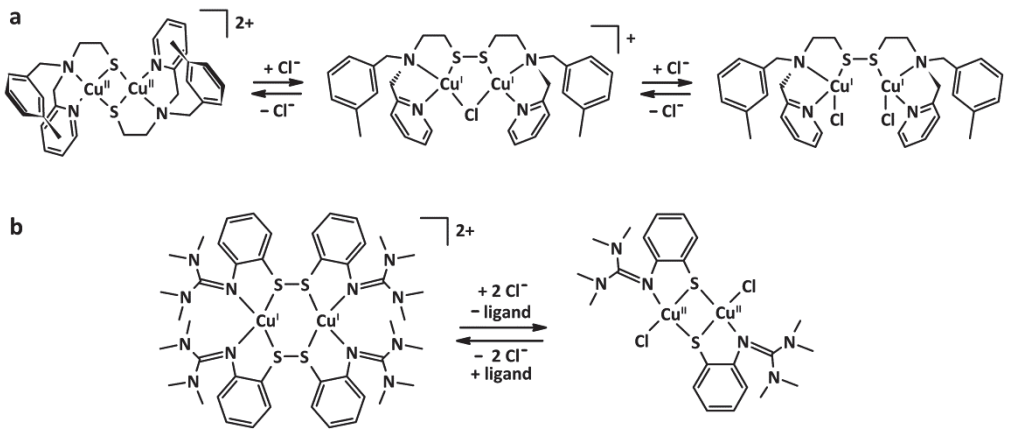

Figure 1.8: Schematic view of the reversible conversion from (a) Cu^{II} thiolate species to Cu^{I} disulfide species[47] and (b) from Cu^{I} disulfide species to Cu^{II} thiolate species[49] upon addition of chloride ions.

The conversion of this Cu^{II} μ-thiolate complex could also be initiated by addition of 2,4-di-*tert*-butylphenolate instead of chloride ions.[64] The authors also briefly mention

that the coordinative properties of the solvent influence the conversion; the use of dichloromethane as a solvent favors the formation of the Cu^{II} μ-thiolate complex while the more strongly coordinating solvent acetonitrile favors the formation of Cu^{I} disulfide species.

A more recent report describes the redox conversion in the opposite direction where a Cu^{I} disulfide complex is converted into a Cu^{II} thiolate complex upon addition of chloride ions in the form of Et_4NCl (Figure 1.8b). The addition of chloride ions leads to dissociation of the ligand thus resulting in tetra-coordinated copper before and after the conversion. The conversion also takes place when bromide ions instead of chloride ions are used and can be reversed by addition of Ag^{+} ions.

1.4.4 Proton-induced conversion

Another interesting example of a Cu^{II} thiolate to Cu^{I} disulfide conversion was published recently.[50] In this paper the conversion is reported to be induced by addition of two equivalents of trifluoridomethanesulfonic acid (HOTf), which results in a color change from dark green to light yellow and disappearance of the Cu^{II} d-d transition bands in the UV-vis absorption spectrum. This reaction can be reversed by addition of N,N-diisopropylethylamine (DIPEA) as depicted in Figure 1.9.

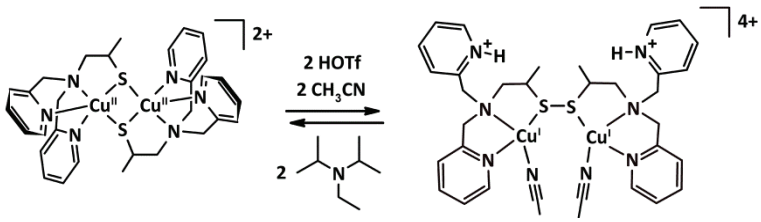

Figure 1.9: Schematic drawing of the conversion of a Cu^{II} thiolate species to a Cu^{I} disulfide species upon addition of HOTf and its reverse reaction by addition of DIPEA.[50]

Protonation of the pyridyl nitrogen of the Cu^{II} thiolate complex is favored over the amine and thiolate moieties, as was determined with ^{1}H NMR NOE enhancements. The presence of Cu^{I} was confirmed with the use of Cu K-edge X-ray Absorbance Spectroscopy.

1.4.5 Thiolate/disulfide equilibrium with cobalt

A similar equilibrium compared to the copper thiolate/disulfide equilibrium was reported for cobalt.[65] The reversible conversion from a mononuclear Co^{III} dithiolate

species to a Co^{II} thiolate/disulfide complex is induced by removal of a chloride ligand by addition of either lithium or silver ions (Figure 1.10)

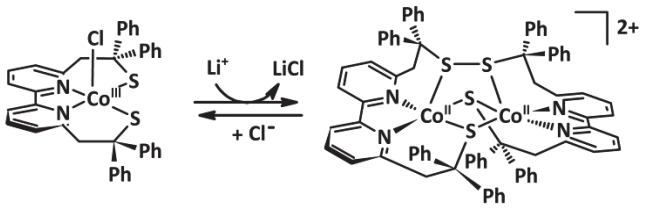

Figure 1.10: Schematic representation of the reversible equilibrium between a Co^{III} thiolate and Co^{II} disulfide complex.[65]

Because of the use of cobalt instead of copper, this conversion can take place under aerobic conditions, which is not the case for the reported copper compounds that can undergo thiolate redox chemistry.

1.5 Aim and outline of this thesis

The focus of the research described in this thesis is on modeling of different aspects of the biomimetic redox reactions between copper ions and sulfur-containing compounds. The dinuclear Cu^{II} μ-thiolate and Cu^{I} disulfide equilibrium can provide a model of the Cu_A site as discussed in section 1.4. As there is limited understanding about why or when Cu^{II} thiolate species form and what determines the conversion to Cu^{I} disulfide complexes the investigations of the effects of small ligand variations on this conversion is described in Chapter 2. Theoretical descriptions of these dinuclear structures are provided, which to the best of our knowledge has not been done before.

In Chapter 3, our investigations of the proton-induced conversion as discussed in section 1.4.4 is reported. The possibility of ligand dissociation instead of conversion to a Cu^{I} disulfide species has been investigated and the experimental results are again supported by DFT calculations.

In Chapter 4, the oxidative degradation of a Cu^{I} thiolate species is described. Oxidation of Cu^{I} thiolate complexes by dioxygen forms a model for possible degradation pathways of copper-sulfur active sites in nature, especially as it is shown that the degradation goes via a Cu^{II} thiolate complex. The Cu^{II} thiolate complex reacts further with dioxygen to form Cu^{II} sulfinate and Cu^{II} sulfonate complexes.

Chapter 5 describes the synthesis of a set of new ligands that are tested for their ability to form Cu^{II} μ-thiolate species. The redox potentials of the Cu^{I} complexes that are formed and crystal structures of Cu^{II} disulfide complexes are discussed.
In Chapter 6, the isolation and analysis of a Cu^{II} phenolate complex is described. This species converts to a Cu^{I} species; a reaction that is reminiscent of the Cu^{II} thiolate to Cu^{I} disulfide conversion. The reaction is of interest since phenols are common substrates in the biological system and are converted to catechols and quinones by copper enzymes (section 1.2.3).
Certain ligands direct copper towards the formation of Cu^{II} μ-thiolate species instead of Cu^{I} disulfide complexes. The copper complexes with these ligands might therefore also stabilize the formation of copper-oxo species, since O and S are in the same group in the periodic table and have similar electron configurations. To test this hypothesis, the reactivity of a large library of Cu^{II} complexes with different ligands have been tested in the oxidation of catechol to *o*-quinone in Chapter 7.
Parts of this thesis have been published,[66-69] are submitted for publication (Chapter 7) or are in preparation for publication (Chapter 6).

1.6 References

1. Solomon, E. I.; Heppner, D. E.; Johnston, E. M.; Ginsbach, J. W.; Cirera, J.; Qayyum, M.; Kieber-Emmons, M. T.; Kjaergaard, C. H.; Hadt, R. G.; Tian, L., *Chem. Rev.* **2014,** *114*, 3659-3853.
2. Mirica, L. M.; Ottenwaelder, X.; Stack, T. D. P., *Chem. Rev.* **2004,** *104*, 1013-1045.
3. Lewis, E. A.; Tolman, W. B., *Chem. Rev.* **2004,** *104*, 1047-1076.
4. Gray, H. B.; Malmstrom, B. G.; Williams, R. J. P., *J. Biol. Inorg. Chem.* **2000,** *5*, 551-559.
5. Solomon, E. I., *Inorg. Chem.* **2006,** *45*, 8012-8025.
6. Solomon, E. I.; Baldwin, M. J.; Lowery, M. D., *Chem. Rev.* **1992,** *92*, 521-542.
7. Solomon, E. I.; Sundaram, U. M.; Machonkin, T. E., *Chem. Rev.* **1996,** *96*, 2563-2605.
8. Koval, I. A.; Gamez, P.; Belle, C.; Selmeczi, K.; Reedijk, J., *Chem. Soc. Rev.* **2006,** *35*, 814-840.
9. Eicken, C.; Krebs, B.; Sacchettini, J. C., *Curr. Opin. Struc. Biol.* **1999,** *9*, 677-683.
10. Randall, D. W.; Gamelin, D. R.; LaCroix, L. B.; Solomon, E. I., *J. Biol. Inorg. Chem.* **2000,** *5*, 16-29.
11. Blackburn, N. J.; de Vries, S.; Barr, M. E.; Houser, R. P.; Tolman, W. B.; Sanders, D.; Fee, J. A., *J. Am. Chem. Soc.* **1997,** *119*, 6135-6143.
12. Savelieff, M. G.; Lu, Y., *J. Biol. Inorg. Chem.* **2010,** *15*, 461-483.
13. Antholine, W. E.; Kastrau, D. H. W.; Steffens, G. C. M.; Buse, G.; Zumft, W. G.; Kroneck, P. M. H., *Eur. J. Biochem.* **1992,** *209*, 875-881.
14. Solomon, E. I.; Xie, X.; Dey, A., *Chem. Soc. Rev.* **2008,** *37*, 623-638.

15. Iwata, S.; Ostermeier, C.; Ludwig, B.; Michel, H., *Nature* **1995,** *376*, 660-669.
16. Tsukihara, T.; Aoyama, H.; Yamashita, E.; Tomizaki, T.; Yamaguchi, H.; Shinzawaitoh, K.; Nakashima, R.; Yaono, R.; Yoshikawa, S., *Science* **1995,** *269*, 1069-1074.
17. Wilmanns, M.; Lappalainen, P.; Kelly, M.; SauerEriksson, E.; Saraste, M., *P. Natl. Acad. Sci. USA* **1995,** *92*, 11955-11959.
18. Brown, K.; Tegoni, M.; Prudencio, M.; Pereira, A. S.; Besson, S.; Moura, J. J.; Moura, I.; Cambillau, C., *Nat. Struct. Biol.* **2000,** *7*, 191-195.
19. Malmstrom, B. G., *J. Biol. Inorg. Chem.* **1998,** *3*, 339-343.
20. Wikstrom, M., *Nature* **1989,** *338*, 776-778.
21. Daskalakis, V.; Pinakoulaki, E.; Stavrakis, S.; Varotsis, C., *J. Phys. Chem. B* **2007,** *111*, 10502-10509.
22. Aoyama, H.; Muramoto, K.; Shinzawa-Itoh, K.; Hirata, K.; Yamashita, E.; Tsukihara, T.; Ogura, T.; Yoshikawa, S., *P. Natl. Acad. Sci. USA* **2009,** *106*, 2165-2169.
23. MacMillan, F.; Kannt, A.; Behr, J.; Prisner, T.; Michel, H., *Biochemistry* **1999,** *38*, 9179-9184.
24. Yu, Y.; Mukherjee, A.; Nilges, M. J.; Hosseinzadeh, P.; Miner, K. D.; Lu, Y., *J. Am. Chem. Soc.* **2014,** *136*, 1174-1177.
25. Wikström, M., *Biochim. Biophys. Acta, Bioenerg.* **2012,** *1817*, 468-475.
26. Gorelsky, S. I.; Ghosh, S.; Solomon, E. I., *J. Am. Chem. Soc.* **2006,** *128*, 278-290.
27. Pomowski, A.; Zumft, W. G.; Kroneck, P. M. H.; Einsle, O., *Nature* **2011,** *477*, 234-237.
28. Ghosh, S.; Gorelsky, S. I.; Chen, P.; Cabrito, I.; Moura, J. J. G.; Moura, I.; Solomon, E. I., *J. Am. Chem. Soc.* **2003,** *125*, 15708-15709.
29. Chan, J. M.; Bollinger, J. A.; Grewell, C. L.; Dooley, D. M., *J. Am. Chem. Soc.* **2004,** *126*, 3030-3031.
30. Ohta, T.; Tachiyama, T.; Yoshizawa, K.; Yamabe, T., *Tetrahedron Lett.* **2000,** *41*, 2581-2585.
31. Bharadwaj, P. K.; Potenza, J. A.; Schugar, H. J., *J. Am. Chem. Soc.* **1986,** *108*, 1351-1352.
32. Bharadwaj, P. K.; John, E.; Xie, C. L.; Zhang, D.; Hendrickson, D. N.; Potenza, J. A.; Schugar, H. J., *Inorg. Chem.* **1986,** *25*, 4541-4546.
33. Houser, R. P.; Tolman, W. B., *Inorg. Chem.* **1995,** *34*, 1632-1633.
34. Coucouvanis, D.; Kanodia, S.; Swenson, D.; Chen, S. J.; Studemann, T.; Baenziger, N. C.; Pedelty, R.; Chu, M., *J. Am. Chem. Soc.* **1993,** *115*, 11271-11278.
35. Aoi, N.; Matsubayashi, G. E.; Tanaka, T., *J. Chem. Soc., Dalton Trans.* **1987**, 241-247.
36. Chadha, R. K.; Kumar, R.; Tuck, D. G., *Can. J. Chem.* **1987,** *65*, 1336-1342.
37. Gómez-Saiz, P.; García-Tojal, J.; Mendia, A.; Donnadieu, B.; Lezama, L.; Pizarro, José L.; Arriortua, Maria I.; Rojo, T., *Eur. J. Inorg. Chem.* **2003,** *2003*, 518-527.
38. Weng, Z.; He, W.; Chen, C.; Lee, R.; Tan, D.; Lai, Z.; Kong, D.; Yuan, Y.; Huang, K.-W., *Angew. Chem. Int. Ed.* **2013,** *52*, 1548-1552.
39. Stange, A. F.; Waldhor, E.; Moscherosch, M.; Kaim, W., *Z. Naturforsch., B: Chem. Sci.* **1995,** *50*, 115-122.

40. Houser, R. P.; Halfen, J. A.; Young, V. G.; Blackburn, N. J.; Tolman, W. B., *J. Am. Chem. Soc.* **1995,** *117*, 10745-10746.
41. Houser, R. P.; Young, V. G.; Tolman, W. B., *J. Am. Chem. Soc.* **1996,** *118*, 2101-2102.
42. Branscombe, N. D. J.; Blake, A. J.; MarinBecerra, A.; Li, W. S.; Parsons, S.; RuizRamirez, L.; Schroder, M., *Chem. Commun.* **1996**, 2573-2574.
43. Uraev, A. I.; Vasilchenko, I. S.; Ikorskii, V. N.; Shestakova, T. A.; Burlov, A. S.; Lyssenko, K. A.; Vlasenko, V. G.; Kuz'menko, T.; Divaeva, L. N.; Pirog, I. V.; Borodkin, G. S.; Uflyand, I. E.; Antipin, M. Y.; Ovcharenko, V. I.; Garnovskii, A. D.; Minkin, V. I., *Mendeleev Commun.* **2005**, 133-135.
44. Rammal, W.; Belle, C.; Beguin, C.; Duboc, C.; Philouze, C.; Pierre, J.-L.; Le Pape, L.; Bertaina, S.; Saint-Aman, E.; Torelli, S., *Inorg. Chem.* **2006,** *45*, 10355-10362.
45. Roy, N.; Sproules, S.; Bothe, E.; Weyhermueller, T.; Wieghardt, K., *Eur. J. Inorg. Chem.* **2009**, 2655-2663.
46. Itoh, S.; Nagagawa, M.; Fukuzumi, S., *J. Am. Chem. Soc.* **2001,** *123*, 4087-4088.
47. Ueno, Y.; Tachi, Y.; Itoh, S., *J. Am. Chem. Soc.* **2002,** *124*, 12428-12429.
48. Raja, D. S.; Bhuvanesh, N. S. P.; Natarajan, K., *Eur. J. Med. Chem.* **2011,** *46*, 4584-4594.
49. Neuba, A.; Haase, R.; Meyer-Klaucke, W.; Flörke, U.; Henkel, G., *Angew. Chem. Int. Ed.* **2012,** *51*, 1714-1718.
50. Thomas, A. M.; Lin, B.-L.; Wasinger, E. C.; Stack, T. D. P., *J. Am. Chem. Soc.* **2013,** *135*, 18912-18919.
51. Gil-Garcia, R.; Fraile, R.; Donnadieu, B.; Madariaga, G.; Januskaitis, V.; Rovira, J.; Gonzalez, L.; Borras, J.; Arnaiz, F. J.; Garcia-Tojal, J., *New J. Chem.* **2013,** *37*, 3568-3580.
52. Ali, M. A.; Mirza, A. H.; Hamid, M. H. S. A.; Aminath, N.; Bernhardt, P. V., *Polyhedron* **2012,** *47*, 79-86.
53. Okamoto, K.; Kuwabara, J.; Kanbara, T., *J. Organomet. Chem.* **2011,** *696*, 1305-1309.
54. Gennari, M.; Pecaut, J.; DeBeer, S.; Neese, F.; Collomb, M.-N.; Duboc, C., *Angew. Chem. Int. Ed.* **2011,** *50*, 5661-5665.
55. Weaver, M. J., *J. Phys. Chem.* **1990,** *94*, 8608-8613.
56. Zhang, S.; Warren, T. H., *Chem. Sci.* **2013,** *4*, 1786-1792.
57. Jacob, C.; Giles, G. L.; Giles, N. M.; Sies, H., *Angew. Chem. Int. Ed.* **2003,** *42*, 4742-4758.
58. Ye, Q.; Imriskova-Sosova, I.; Hill, B. C.; Jia, Z., *Biochemistry* **2005,** *44*, 2934-2942.
59. Cawthorn, T. R.; Poulsen, B. E.; Davidson, D. E.; Andrews, D.; Hill, B. C., *Biochemistry* **2009,** *48*, 4448-4454.
60. Banci, L.; Bertini, I.; Cavallaro, G.; Ciofi-Baffoni, S., *Febs Journal* **2011,** *278*, 2244-2262.
61. Jacobson, R. R.; Tyeklar, Z.; Farooq, A.; Karlin, K. D.; Liu, S.; Zubieta, J., *J. Am. Chem. Soc.* **1988,** *110*, 3690-3692.
62. Hayashi, H.; Fujinami, S.; Nagatomo, S.; Ogo, S.; Suzuki, M.; Uehara, A.; Watanabe, Y.; Kitagawa, T., *J. Am. Chem. Soc.* **2000,** *122*, 2124-2125.
63. Kieber-Emmons, M. T.; Ginsbach, J. W.; Wick, P. K.; Lucas, H. R.; Helton, M. E.; Lucchese, B.; Suzuki, M.; Zuberbühler, A. D.; Karlin, K. D.; Solomon, E. I., *Angew. Chem. Int. Ed.* **2014,** *53*, 4935-4939.

64. Osako, T.; Ueno, Y.; Tachi, Y.; Itoh, S., *Inorg. Chem.* **2004,** *43*, 6516-6518.
65. Gennari, M.; Gerey, B.; Hall, N.; Pécaut, J.; Collomb, M.-N.; Rouzières, M.; Clérac, R.; Orio, M.; Duboc, C., *Angew. Chem.* **2014,** *126*, 5422-5425.
66. Ording-Wenker, E. C. M.; Siegler, M. A.; Lutz, M.; Bouwman, E., *Inorg. Chem.* **2013,** *52*, 13113-13122.
67. Ording-Wenker, E. C. M.; van der Plas, M.; Siegler, M. A.; Bonnet, S.; Bickelhaupt, F. M.; Fonseca Guerra, C.; Bouwman, E., *Inorg. Chem.* **2014,** *53*, 8494-8504.
68. Ording-Wenker, E. C. M.; van der Plas, M.; Siegler, M. A.; Fonseca Guerra, C.; Bouwman, E., *Chem. Eur. J.* **2014,** *20*, 16913-16921.
69. Ording-Wenker, E. C. M.; Siegler, M. A.; Bouwman, E., *Inorg. Chim. Acta* **2015,** *in press*.